

# Series expansion and computer simulation studies of random sequential adsorption

Jian-Sheng Wang  
Department of Computational Science,  
National University of Singapore,  
Singapore 119260, Republic of Singapore

8 March 1999

## Abstract

We discuss two important techniques, series expansion and Monte Carlo simulation, for random sequential adsorption study. Random sequential adsorption is an idealization for surface deposition where the time scale of particle relaxation is much longer than the time scale of deposition. Particles are represented as extended objects which are adsorbed to a continuum surface or lattice sites. Once landed on the surface, the particles stick to the surface. We review in some details various methods of computing the coverage  $\theta(t)$  and present some of the recent and new results in random sequential adsorption.

## 1 Random sequential adsorption problem

The random sequential adsorption (RSA) problem arises from a number of situations in physics, chemistry, and biology. One of the early RSA problem comes from polymer chemistry. Flory [1] was interested in the dimerization of polymer chain. The adjacent monomers on the side of the chain form dimers one at a time until no pair of monomers is available. He found the final reacted monomers based purely on geometric argument. It turns out that this problem is equivalent to a random sequential adsorption of dimers on a one-dimensional lattice. Consider the one-dimensional lattice, with all sites empty initially. At time  $t > 0$ , dimers, each of which occupies two consecutive sites, are dropped on the lattice at a rate  $k$  per second equally likely at any locations (see Fig. 1(a)). As long as the two sites are empty, a dimer lands on the lattice. If any one of the two sites is already occupied, the deposition is rejected. This is the basic RSA model.

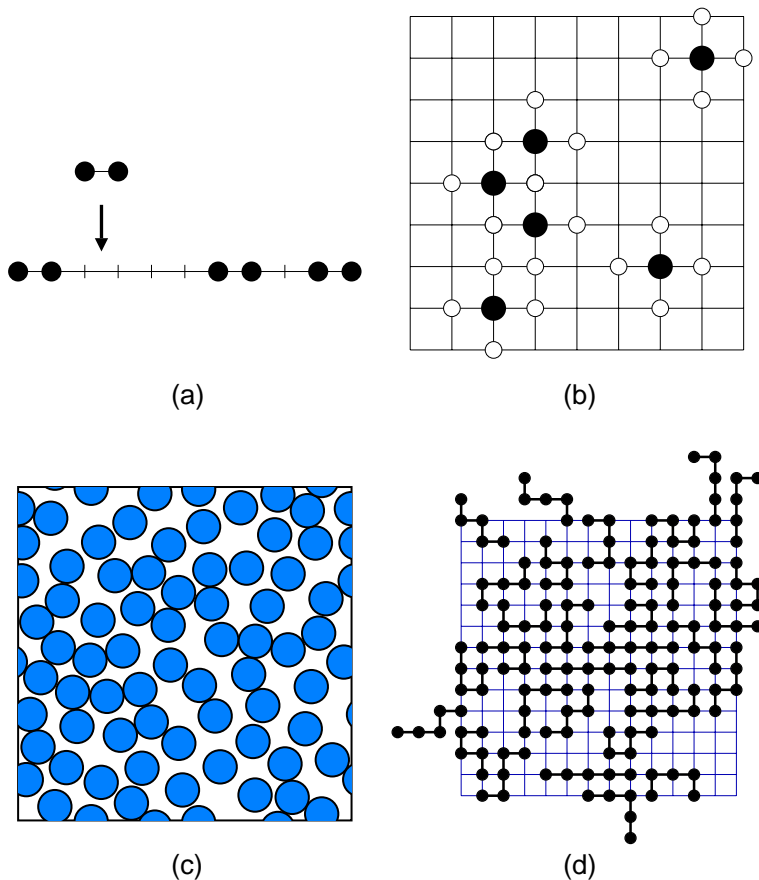


Figure 1: Some typical random sequential adsorption configurations. (a) Dimer deposition on a one-dimensional lattice; (b) monomer with nearest neighbor exclusion; (c) the jamming state of hard discs on continuum; (d) self-avoiding random walks of length  $N = 5$  on square lattice.

RSA of many different geometric objects has been studied. The deposition of unit line segments on a one-dimensional continuum is called car-parking problem [2]. The deposition of discs on two-dimensional continuum [3] is relevant to the adsorption of colloids or protein molecules on glass surface [4, 5]. Lattice models of various geometries are studied. In Fig. 1 we show some typical configurations of RSA models.

The very basic question of RSA is the time dependence of the coverage,  $\theta(t)$ , and the jamming coverage,  $\theta(\infty)$ . The approach to the jamming coverage is also of considerable interest. It turns out that the approach to the jamming coverage is to some extent universal. For lattice models, the approach to jamming is always exponential due to the discreteness of the problems [6], while for continuum problems the asymptotic dependences exhibit power laws which depend on the symmetry of the deposited objects [7, 8, 9, 10].

A comprehensive review on RSA and cooperative sequential adsorptions is given by Evans [11]. Bartelt and Privman [12] reviewed, among other things, mean-field approximations. Progress on experiment work is given by Ramsden [13]. Random sequential adsorption has many aspects and is rich with problems. In this article, we limit our scope to consider two important approximate techniques for computing the coverage of RSA. They are the series expansion and Monte Carlo simulation. The emphasis is on methods rather than specific results. Only one-dimensional problems [14, 15, 16, 17, 18] and quasi-one-dimensional problems [19, 20, 21] have exact solutions. Two-dimensional problems are most likely intractable. Because of this, the approximate methods like series expansion and Monte Carlo are very useful for the study of RSA. We present some of the technical details which are usually given only briefly in original research papers. With examples, we show how the series can be obtained and analyzed with Padé approximation. For Monte Carlo simulation, the emphasis is on efficient algorithms for RSA simulation.

## 2 Series expansions

One of the well-developed methods in studying random sequential adsorption is series expansion around time  $t = 0$ . The method gains experience from series expansion studies of other problems in condensed matter physics [22]. Series expansion approach was the only successful method to obtain nonclassical results in the study of critical phenomena for a while before the advent of renormalization group method [23]. The methods and technique developed, especially the Padé approximation technique [24], have been also applied successfully to random sequential adsorption. The technique offers a systematic approach with controlled approximation. Unlike the approach with truncated rate equations [25, 26, 27], series expansion can be automated on computer relatively easily, and the number of terms obtained can be rather high. In many cases, the accuracy is higher than or comparable to most accurate Monte Carlo simulation results.

The series expansion for the rate of adsorption as a function of particle density has been introduced by Widom [28]. It was shown that this type of expansion is similar to virial expansion for the equation of state. In fact, the first two coefficients involving one and two-particle distributions are the same. The difference between equilibrium system and RSA starts at third order. Series for hard discs on two-dimensional continuum up to third order were first obtained by Schaaf and Talbot [29]. Series expansions for lattice models and continuum systems have been considered by Hoffman [30] and Evans [31]. Evans presented rate equation approach for deriving series. The series in time and in density are related by a transformation, so they are equivalent. High-order series with the help of computer were derived by Baram and Kutasov [32], Dickman *et al* [33], Bonnier *et al* [34], Baram and Fixman [35], and Gan and Wang [36].

## 2.1 Rate equations

The RSA process can be described fully with a master equation of the form

$$\frac{\partial P(\{\sigma\}, t)}{\partial t} = \sum_{\{\sigma'\}} \Gamma(\{\sigma\}, \{\sigma'\}) P(\{\sigma'\}, t), \quad (1)$$

where  $\{\sigma\}$  is a set of state variables which completely specify the state of the system;  $P(\dots)$  is the probability of such a state; and  $\Gamma$  is a transition matrix. For notational convenience, we shall consider discrete lattice models. Continuous space problem can be generalized easily. Then  $\{\sigma\}$  denotes a set of occupation variables  $\sigma_i$  located at site  $i$ .

Although Eq. (1) contains the complete information of the process, it is rather difficult to deal with efficiently due to the high dimensionality of the problem. Thus, in most of the analytic treatments, reduced quantities are worked with. One of the most important such quantities is the marginal probability distribution:

$$P(G) = \sum_{\{\sigma\}, \sigma_i = \sigma_i^0 \text{ for } i \in G} P(\{\sigma\}), \quad (2)$$

where the summation is over all the possible states such that a given set  $G$  of sites takes a known set of values. That is,  $P(G)$  is the probability that a given set of sites having specified values. For the standard RSA problem, it is sufficient to consider only a set of connected sites which are unoccupied.

Our task is to write down a set of differential equations for  $P(G)$ . In principle, we can derive them from the master equation (1). This is not really necessary, and we can give the equations based on physical meaning of  $P(G)$ . Let us take a look of the equations associated with a random sequential deposition of dimers on a one-dimensional lattice. In this case, we consider the probability  $P_n$  that a consecutive  $n$  sites are empty. Assuming translational invariance of the initial conditions, this probability does not depend on the specific locations. Due to the simple geometry in one dimension, the set  $G$  of  $n$  connected sites being empty can be characterized by a single integer  $n$ . Let us consider the change of  $P_n$  by the deposition process. We assume that the  $n$  empty sites are at  $i = 1, 2, \dots, n$ . Clearly, depositions of dimers involving the sites  $i \leq 0$  or  $i > n$  do not change  $P_n$ , while depositions inside empty sites on 1 to  $n$  destroy the consecutive empty sequence, the probability of which is proportional to  $P_n$  for each of the  $n - 1$  possible ways of depositions. At the two ends, the empty sequence can be destroyed with one site at 0 (or  $n + 1$ ) outside the sequence and the other site at 1 (or  $n$ ) in the sequence, see Fig. 2. In order for this to happen, the site just outside the considered sequence should be empty, the probability of which is  $P_{n+1}$ . There are two ways to do this. Putting all these together, we have,

$$-k^{-1} \frac{dP_n(t)}{dt} = (n - 1)P_n(t) + 2P_{n+1}(t), \quad n = 1, 2, 3, \dots \quad (3)$$

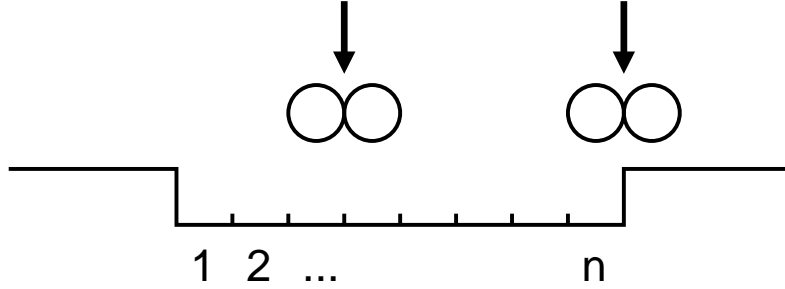


Figure 2: The one-dimensional dimer deposition. The sites 1 to  $n$  are known to be empty, but the status of other sites are unknown.

The proportionality constant  $k$  sets the time scale. Without loss of generality, we can take it to be unity. This equation can be solved [16] to give

$$P_n(t) = \exp[-(n-1)t - 2 + 2e^{-t}]. \quad (4)$$

Note that the coverage is just  $\theta(t) = 1 - P_1(t)$ .

Similar consideration gives so-called rate equations [37] for other deposition processes. For example, in deposition of dimers on square lattice, the basic quantity of interest is the probability  $P(G)$  that the given set  $G$  of sites are empty; we do not care other sites being occupied or empty. The rate of decrease is proportional to the probability that the current configuration  $G$  can be destroyed by depositing a dimer with at least one site in  $G$ . Thus we have

$$-\frac{dP(G)}{dt} = \sum_{\text{ways of destroying } G} P(G'), \quad (5)$$

where the summation runs over all possible ways of depositing a dimer at a pair of empty sites such that at least one site is in  $G$ ;  $G' = G$  if two of the dimer sites of a deposition attempt are within  $G$ , or  $G'$  is one site more than  $G$  so that a deposition with one site in  $G$  and one site outside  $G$  can be carried out. The first two equations look like these:

$$-\frac{dP(o)}{dt} = 4P(oo), \quad (6)$$

$$-\frac{dP(oo)}{dt} = P(oo) + 2P(ooo) + 4P(o\overset{O}{oo}). \quad (7)$$

There are four ways to destroy a single empty site, provided that the nearest neighbor site is also empty. Using the assumption that initial conditions are lattice symmetry invariant, we can write them simply as  $4P(oo)$ . The second equation is derived similarly.

For a general discussion, we write the rate equations symbolically as

$$\frac{dP(G)}{dt} = \mathcal{L}P(G), \quad (8)$$

where  $\mathcal{L}$  is a linear operator defined by

$$\mathcal{L}P(G) = \sum_{G'} c_{G'} P(G'). \quad (9)$$

The  $n$ -th derivative is then

$$\frac{d^n P(G)}{dt^n} = \mathcal{L}^n P(G), \quad \text{with} \quad P(G)|_{t=0} = 1 \quad \text{for all } G. \quad (10)$$

We assume that all sites are empty at  $t = 0$ .

## 2.2 Simple counting methods for lattice models

We can obtain the rules for series expansion starting from the rate equation, Eq. (8). We begin with a concrete example of the random sequential adsorption of single site occupation with nearest neighbor exclusion on a square lattice. A site can be occupied by a particle, as long as the four nearest neighbors are empty. Figure 1(b) shows a sample configuration of the nearest neighbor exclusion RSA model.

The first few rate equations read:

$$-\frac{dP(\text{o})}{dt} = P\left(\begin{array}{c} \text{o} \\ \text{o} \end{array}\right), \quad (11)$$

$$-\frac{d}{dt}P\left(\begin{array}{c} \text{o} \\ \text{o} \end{array}\right) = P\left(\begin{array}{c} \text{o} \\ \text{o} \end{array}\right) + 4P\left(\begin{array}{cc} \text{o} & \text{o} \\ \text{o} & \text{o} \end{array}\right), \quad (12)$$

$$-\frac{d}{dt}P\left(\begin{array}{ccc} \text{o} & \text{o} & \text{o} \\ \text{o} & \text{o} & \text{o} \end{array}\right) = 2P\left(\begin{array}{ccc} \text{o} & \text{o} & \text{o} \\ \text{o} & \text{o} & \text{o} \end{array}\right) + 2P\left(\begin{array}{ccc} \text{o} & \text{o} & \text{o} \\ \text{o} & \text{o} & \text{o} \end{array}\right) + 4P\left(\begin{array}{ccc} \text{o} & \text{o} & \text{o} \\ \text{o} & \text{o} & \text{o} \end{array}\right), \quad (13)$$

where a pattern with o's denotes a set of sites of that geometric arrangement which are empty (while other sites are unspecified). We have taken into account the translational and rotational symmetry of the problem. The equations are generated as follows. For each given configuration  $G$ , we consider all possible ways of destroying the configuration by a deposition of a particle at each one of the empty sites. If the four neighbors are already known to be empty, the rate is simply proportional to the original probability  $P(G)$ . If the site is adjacent to sites of unknown status, we require those sites to be empty. Thus this second type of process creates new configurations  $G'$  which have more empty sites than  $G$ .

From this set of rate equations we can get the  $n$ -th derivative of the probability that the sites in the set  $G$  are empty,  $P^{(n)}(G) = d^n P(G)/dt^n|_{t=0}$ . With an initial condition of empty lattice at  $t = 0$ , the zeroth derivative  $P(G, t = 0)$  equals 1 for all configurations  $G$ . The most relevant one is the probability that a single site is empty,  $P(\text{o}, t)$ , since  $\theta(t) = 1 - P(\text{o}, t)$  is the coverage. Power series expansion is obtained from the derivatives evaluated at  $t = 0$ :

$$P(\text{o}, t) = \sum_{n=0}^{\infty} P^{(n)}(\text{o}) \frac{t^n}{n!}. \quad (14)$$

For the nearest neighbor exclusion model, we have  $P(o) = 1$ .  $P'(o) = -1$  from Eq. (11). From Eq. (11) and (12), we get  $P''(o) = -P'(\overset{o}{\underset{o}{\text{oo}}}) = P(\overset{o}{\underset{o}{\text{oo}}}) + 4P(\overset{oo}{\underset{oo}{\text{oooo}}}) = 5$ . Similarly, we find  $P'''(o) = -P''(\overset{o}{\underset{o}{\text{oo}}}) = P'(\overset{o}{\underset{o}{\text{oo}}}) + 4P'(\overset{oo}{\underset{oo}{\text{oooo}}}) = -37$ . Thus, to third order, the expansion is

$$P(o, t) = 1 - t + \frac{5}{2}t^2 - \frac{37}{6}t^3 + O(t^4). \quad (15)$$

The process of obtaining the answer can be thought as counting the number of patterns in  $n$  generations. We note that for each current configuration  $G$ , we go over the sites of  $G$  once, each generated a next generation pattern, which may or may not be the same as the parent pattern. The expansion coefficient  $S(n) = (-1)^{(n+1)}d^{n+1}P(o, t)/dt^{n+1}|_{t=0}$  is simply the total number of possible patterns (or sequences), where two-dimensional coordinate  $x_0 = (0, 0)$  is fixed at the origin, while  $x_1$  varies in a domain  $D(x_0)$ , and  $x_2$  in a union domain  $D(x_0) \cup D(x_1)$ ,  $\dots$ , and  $x_n$  varies in a domain  $D(x_0) \cup D(x_1) \cdots \cup D(x_{n-1})$ . The domain  $D(x)$  is the center site  $x$  plus four nearest neighbor sites of  $x$ . We write [33]

$$S(n) = \sum_{x_1 \in D(x_0)} \sum_{x_2 \in D(x_0) \cup D(x_1)} \cdots \sum_{x_n \in D(x_0) \cup D(x_1) \cdots \cup D(x_{n-1})} 1. \quad (16)$$

$S(0)$  is defined by  $-dP(o, t)/dt|_{t=0}$ . By definition,  $S(n)$  is always positive. In terms of  $S(n)$ , the expansion for the rate of adsorption is

$$\phi = -\frac{dP(o, t)}{dt} = \sum_{n=0}^{\infty} S(n) \frac{(-t)^n}{n!}. \quad (17)$$

This notation is convenient, for Eq. (16) generalizes to other type of lattice models by choosing a different domain  $D(x)$  and generalizes to random sequential adsorption on continuum. For anisotropic objects,  $x$  should be understood as position and orientation as well.

The easiest way of implementing this counting method is to use recursive function calls. Consider the following C-like pseudo-code:

```

RSA( $G, n$ )
{
   $S(n) += |G|$ ;
  if ( $n \geq N_{max}$ ) return;
  for each ( $x \in G$ ) {
    RSA( $G \cup D(x), n + 1$ );
  }
}

```

In this program,  $G$  is a set of empty sites, which can be represented by a list of coordinates of the sites;  $G \cup D(x)$  is the union of the set  $G$  and the set consisting of

$x$  and its four nearest neighbors;  $|G|$  is the cardinality of the set. The variable  $G$  is local to each function call, while  $S(n)$  is global. We assume that  $S(n)$  is initialized to zero. The recursion stops after  $N_{max}$  in depth, which gives us results for  $S(0)$  to  $S(N_{max})$ . If we evoke the program by  $\mathbf{RSA}(G, 0)$ , the derivatives  $d^n P(G)/dt^n|_{t=0} = (-1)^n S(n-1)$ ,  $1 \leq n \leq N_{max} + 1$ , are computed.

Clearly, the above algorithm can be improved. First of all, we need not count a configuration if it is the same as the parent configuration. We shall discuss this in detail later in Section 2.5. The second improvement is to rewrite the recursive calls by nonrecursive procedure. Since the set  $G$  always contains the parent set where  $G$  is derived, it is possible to use only one list representing all the  $G$ 's (one for each level in the recursion), each ends at some point in the list. Of course, the bookkeeping will be more complicated. None of the above suggestions will improve the speed of calculation substantially. In next section, we discuss perhaps the most efficient algorithm [38] for the series expansions on lattices.

## 2.3 More advanced methods

We note that in the simple counting algorithm, we did not use the symmetry of the problem. Two patterns related by translation or rotation symmetry should have the same derivatives, but this is not recognized. In order to exploit fully the symmetry of the problem, we use the technique of dynamic programming, and use sophisticated data structures. The starting point is again the rate equation, Eq. (8). It turns out that the best algorithm is to combine this method with a simple counting algorithm.

A general function is coded which returns the right-hand side of Eq. (8) when the configuration  $G$ , or the set  $G$ , is given. The set  $G$  is represented as a list of coordinates constructed in an ordered manner. Note that each term on the right-hand side of the equation is just the probability of the set  $G \cup D(x)$  being empty, where  $x$  runs over the sites of  $G$ . Terms which are identical after translational and rotational symmetry consideration are collected as one term with associated coefficients. Each rate equation is represented by a node together with a list of pointers to other nodes. Each node represents a function characterized by the set  $G$ . The node contains pointers to the derivatives of this node obtained so far, and pointers to the ‘‘children’’ of this node and their associated coefficients, which form a symbolic representation of the rate equations. The computation of  $n$ -th derivative uses the rate equations recursively. Since each node is linked to other nodes, the computation of the  $n$ -th derivative can be considered as expanding a ‘‘tree’’ (with arbitrary number of branches) of depth  $n$ . The tree structure for the nearest neighbor exclusion model is shown in Fig. 3. Unlike the standard tree, we allow loops linking back to earlier generations.

The traversal or expansion of the tree [39] can be done in a depth-first fashion or a breadth-first fashion. Each has a different computational complexity. A simple depth-first traversal requires only a small amount of memory of order  $n$ . However,



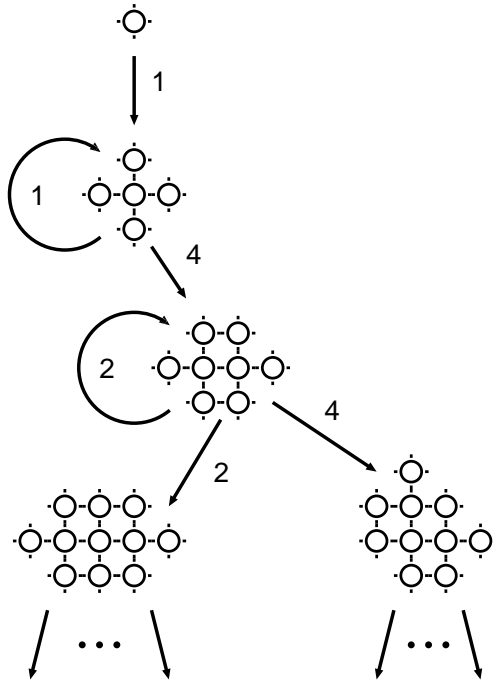


Figure 3: The “tree” structure representing Eq. (11) to (13) in the RSA series expansion of the monomer with nearest neighbor exclusion. The arrows point from parent to child generations; the numbers indicate the expansion coefficients (number of equivalent patterns).

the time complexity is at least exponential,  $b^n$ , with a large base  $b$ . A breadth-first algorithm consumes memory exponentially, even after the number of the rate equations has been reduced by taking the symmetry of the problem into account. The idea of dynamic programming can be incorporated in the breadth-first expansion where the intermediate results are stored and referred. To achieve the best performance, a hybrid of strategies is used to reduce the computational complexity:

- Each configuration (pattern) is transformed into its canonical representation; all configurations related by lattice symmetry are considered as the same configuration.
- We use breadth-first expansion to avoid repeated computations involving the same configuration. If a configuration has already appeared in earlier expansion, a pointer reference is made to the old configuration. Each configuration is stored in memory only once. However, storing of all the distinct configurations leads to a very fast growth in memory consumption. For a quick check if a configuration is already stored, we use the standard technique of hashing [39].
- The last few generations in the tree expansion use a simple depth-first traversal

to curb the problem of memory explosion.

- Parallel computation proves to be useful.

The program is controlled by two parameters  $D$  and  $C$ .  $D$  is the depth of breadth-first expansion of the tree. When depth  $D$  is reached, we no longer want to continue the normal expansion in order to conserve memory. Instead, we consider each leaf node afresh as the root of a new tree. The derivatives up to  $(n - D)$ th order are computed for this leaf node. The expansions of the leaf nodes are done in serial, so that the memory resource can be reused. The parameter  $C$  controls the number of last  $C$  generations which should be computed with a simple depth-first expansion algorithm. It is a simple recursive counting algorithm, which uses very little memory, and can run fast if the depth  $C$  is not very large. In this algorithm the lattice symmetry is not treated.

This technique is used to obtain the RSA series for dimer and nearest neighbor exclusion models on square and honeycomb lattices [36], RSA with diffusional relaxation [40], and Ising relaxation dynamics [41].

## 2.4 Series for continuum systems

The results derived for lattice model can be generalized for continuum system. Consider the deposition of disc of diameter  $\sigma = 1$ . One way to obtain the rules for series expansion in continuum is to consider the limit of discretized lattice model. The RSA of discs can be thought as approximate lattice problem with a single-site deposition and exclusion of sites within some distance of the occupied site. The analog of Eq. (16) is [33],

$$S(n) = \int_{x_1 \in D(x_0)} dx_1 \int_{x_2 \in D(x_0) \cup D(x_1)} dx_2 \cdots \int_{x_n \in D(x_0) \cup D(x_1) \cdots \cup D(x_{n-1})} dx_n, \quad (18)$$

where  $x_i$  is interpreted as a  $d$ -dimensional vector,  $dx_i$  is a  $d$ -dimensional volume element, and  $x \in D(x_i)$  is the set such that  $|x - x_i| \leq 1$ .

The integral in Eq. (18) has a rather complicated integration domain. To simplify the integral, we introduce the ‘‘Mayer function’’ of a hard disc system,

$$f_{ij} = f(x_i - x_j) = \begin{cases} -1, & \text{if } |x_i - x_j| \leq 1; \\ 0, & \text{otherwise.} \end{cases} \quad (19)$$

Then we can rewrite the integral with integration domain in the whole space and with the integrand consisting of terms of products of  $f_{ij}$ :

$$-S(1) = \int f_{01} dx_1, \quad (20)$$

$$S(2) = \int f_{01} dx_1 \int [f_{02} + f_{12}(1 + f_{02})] dx_2, \quad (21)$$

and in general

$$(-1)^n S(n) = \int dx_1 \int dx_2 \cdots \int dx_n \prod_{k=1}^n \left( \sum_{j=0}^{k-1} f_{jk} \prod_{i=0}^{j-1} (1 + f_{ik}) \right). \quad (22)$$

The result of expanding the terms leads to the following graph-theoretic description:  $(-1)^n S(n)$  is the sum of the contributions from all connected  $(n+1)$ -point unlabeled graphs; each term is the value of an integral associated with the graph times an integer multiplicity factor. The value of a (labeled) graph is the integral of a form  $\int \cdots \int dx_1 dx_2 \cdots dx_n \prod f_{ij}$ , called cluster integral. The numerical factor is the number of topologically distinct ways of labeling the graph, subject to the following constraint: the labels are put down in sequential order from 0 to  $n$ , such that the current vertex  $k$  is connected to a vertex  $j < k$ . There is a one-to-one correspondence between a graph and an integral. Each vertex  $i$  of the graph corresponds to an integration variable  $x_i$  (except vertex 0), and each edge  $(i, j)$  of the graph corresponds to a function  $f_{ij}$ . The definitions differ slightly from the normal convention [42]. The diagrammatic rules give, for the particle density, the following expression for the first few terms,

$$\begin{aligned} \rho(t) = & t + (o-o) \frac{t^2}{2!} + \left( 2 \begin{array}{c} \circ \\ | \\ \circ-o \end{array} + \begin{array}{c} \circ \\ \diagdown \diagup \\ \circ-o \end{array} \right) \frac{t^3}{3!} + \\ & \left( 2 \begin{array}{c} \circ \\ | \\ \circ-o \end{array} \begin{array}{c} \circ \\ | \\ \circ-o \end{array} + 4 \begin{array}{c} \circ \\ | \\ \circ-o \end{array} \begin{array}{c} \circ \\ | \\ \circ-o \end{array} + 7 \begin{array}{c} \circ \\ \diagdown \diagup \\ \circ-o \end{array} + 2 \begin{array}{c} \circ-o \\ | \\ \circ-o \end{array} + 5 \begin{array}{c} \circ-o \\ | \\ \circ-o \end{array} + \begin{array}{c} \circ-o \\ \diagdown \diagup \\ \circ-o \end{array} \right) \frac{t^4}{4!} + O(t^5). \end{aligned} \quad (23)$$

This diagrammatic rule is similar to the Mayer theory [42, 43] for equilibrium fluid system. The major difference is the prefactor. In Mayer theory, the integer factor is simply the number of different ways of labeling a graph, without imposing an ordering. It turns out that the parallel is deeper than this, see Table 1. Just like the topological reduction in Mayer theory, by some transformation, Given [44] arrived at an expansion involving only the star graphs (irreducible graphs). Let  $\phi = d\rho/dt$  be the rate of adsorption, which is proportional to the area available for deposition. We have the following virial expansion

$$\ln \phi = \sum_{n=1}^{\infty} b_n \frac{\rho^n}{n!}, \quad (24)$$

where  $b_n$  is the sum of contributions from all  $(n+1)$ -point star graphs with the RSA multiplicity factor. The first few terms are

$$\ln \phi = (o-o)\rho + \left( \begin{array}{c} \circ \\ \diagdown \diagup \\ \circ-o \end{array} \right) \frac{\rho^2}{2!} + \left( 2 \begin{array}{c} \circ-o \\ | \\ \circ-o \end{array} + 5 \begin{array}{c} \circ-o \\ | \\ \circ-o \end{array} + \begin{array}{c} \circ-o \\ \diagdown \diagup \\ \circ-o \end{array} \right) \frac{\rho^3}{3!} + O(\rho^4). \quad (25)$$

The diagrammatic rules can also be applied to lattice models when the Mayer function and integrals are properly interpreted. In fact, Hoffman [30] has derived a

expansion variable	fugacity $z$	time $t$
quantities	pressure $\beta P = \frac{\ln \Xi}{V}$ $\phi^{eq} = \frac{\rho}{z} = \frac{1}{V} \frac{d \ln \Xi}{dz}$	density $\rho$ adsorption rate $\phi = \frac{d\rho}{dt}$
basic expansion	$\beta P = \frac{\ln \Xi}{V} = \sum_{n=1}^{\infty} a_n \frac{z^n}{n!}$	$\rho = \sum_{n=1}^{\infty} a_n \frac{t^n}{n!}$
graphs	$a_n =$ sum of all topologically distinct, labeled, connected $n$ -point graphs.	$a_n =$ sum of all topologically distinct, labeled, connected $n$ -point graphs, subject to the labeling constraint that a vertex $i$ must be connected to a vertex with label less than $i$ .
virial expansion	$\ln \phi^{eq} = \ln \frac{\rho}{z} = \sum_{n=1}^{\infty} b_n \frac{\rho^n}{n!}$	$\ln \phi = \sum_{n=1}^{\infty} b_n \frac{\rho^n}{n!}$
topological reduction	$b_n =$ sum of all topologically distinct, labeled, doubly connected (irreducible) $(n+1)$ -point graphs. $\beta P = \rho - \sum_{n=1}^{\infty} \frac{b_n}{n+1} \frac{\rho^{n+1}}{(n-1)!}$ .	$b_n =$ sum of all topologically distinct, labeled, doubly connected (irreducible) $(n+1)$ -point graphs, subject to the labeling constraint that a vertex $i$ must be connected to a vertex with label less than $i$ .

Table 1: Comparison of equilibrium Mayer expansion and random sequential adsorption.

similar expansion for a lattice cooperative sequential adsorption model, while Tarjus *et al* [45] obtained diagrammatic expansion from a very different method.

The computation of the cluster integrals can be further simplified by noting that if a connected graph can be decomposed into several star graphs, the value of the connected graph is equal to the products of the values of star graphs. Because of this, we need only to evaluate the values of star integrals. An articulation point is a vertex belonging to the graph, such that when this vertex and its connecting edges are removed, the graph becomes disconnected. A star graph does not have an articulation point. The decomposed graphs of a connected graph are two or more graphs with the articulation point duplicated in each of the separated graphs when the articulation point is removed, with the edges still attached to the graphs. Figure 4 demonstrates some of the concepts.

In the work of Dickman *et al* [33], the series were obtained this way, using the existing cluster integrations in the fluid Mayer expansion. For the deposition of discs, the series was obtained up to  $S(4)$ . For the squares of fixed orientation, the series is based on the result of one-dimensional cluster integrals [46] which were already

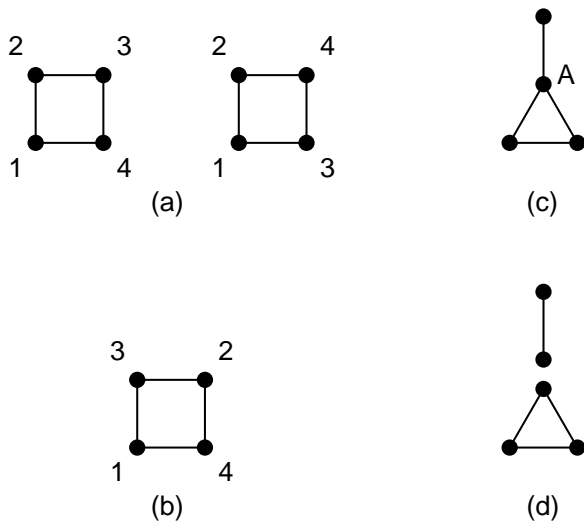


Figure 4: Some concepts of graph theory: (a) The labeling of the vertices consistent with RSA constraints; (b) this graph appears in equilibrium theory but not in RSA; (c) a connected graph with an articulation point, labeled A; (d) the connected graph (c) is decomposed into two star graphs (irreducible graphs).

computed as early as in 1962 up to order 6. Note that for oriented hypercubes in  $d$  dimensions, a cluster integral is equal to the one-dimensional cluster integral raised to the power  $d$ . This fact was used to obtain two-dimensional results. Bonnier *et al* [34] obtained results for  $d = 2, 3$ , and 4 for RSA of oriented squares, cubes, and hypercubes, using an extrapolation procedure from a lattice to continuum. In Table 2 we collect some of the series coefficients.

The computational complexity of the RSA on continuum is perhaps more than  $(n!)^3$ . One algorithm that we have implemented in this work consists of two steps. The first step reduces the labeled graphs to unlabeled graphs, directly from defining Eq. (22). This gives us the RSA topologically distinct labeling factor. This step is purely graph-theoretic, and is independent of the detail of the problem. There are  $\prod_{k=1}^n (2^k - 1) = O(2^{n^2/2})$  labeled graphs at order  $n$ . To reduce the graphs to unlabeled graphs, we consider all the  $n$  factorial possible permutations of the labels, taking the “largest one” as the canonical representation of the (unlabeled) graph. The largest one is the one with incidence matrix viewed as a big binary integer giving biggest value. Since there are  $O(2^{n^2/2})$  graphs, each needs  $n!$  transformations, the overall time complexity is  $O(2^{n^2/2}n!)$ . The above step reduces the number of graphs by a factor of about  $1/n!$ . Much fast algorithms exist which generate each unlabeled graph exactly once. We used McKay’s `geng` program [47], which greatly speeds up this part of the computation.

The second step is to compute the integrals. computation of the cluster integrals can be done exactly for the discs only for  $n \leq 3$ . For the one-dimensional segments, it can be done in time of  $O(n^4n!)$ . The result raised to the  $d$ -th power

n	hard disc	oriented square	nearest neighbor exclusion
0	1	1	1
1	2	4	5
2	$4 + 3\sqrt{3}/\pi$	23	37
3	$8 + 14\sqrt{3}/\pi + 44/\pi^2$	168	349
4	86.02824	$\frac{105895}{72}$	3925
5		$\frac{6709687}{450}$	50845
6		$\frac{1385692277}{8100}$	742165
7		$\frac{867234755659}{396900}$	12017245
8		$\frac{7953008984179}{259200}$	213321717
9			4113044061
10			85493084853
11			1903886785277
12			45187885535477
13			1137973688508989
14			30289520203949205
15			849248887429012733
16			25007259870924817749
17			771322713104711008093
18			24860884250598911650645
19			835568036857675195155997
20			29227671255970830546587445

Table 2: The series expansion coefficient  $S(n)$  for the hard discs [33], oriented squares [this work], and nearest neighbor exclusion on square lattice [36].

gives the  $d$ -dimensional hypercubic result. For a given cluster integral, the set of  $f_{ij}$  gives a set of constraints. The integral is in fact equal to the volume of a convex polygon in an  $n$ -dimensional space. This  $n$ -dimensional space is partitioned into  $n!$  regions, characterized by  $x_{i_1} < x_{i_2} < \dots < x_{i_n}$  where  $(i_1, i_2, \dots, i_n)$  is a permutation of  $(1, 2, \dots, n)$ . Once this extra constraint is given, the integration limits can be written down explicitly [46]. The integrals in each sector can be evaluated symbolically in polynomial time.

This latest program gives only two extra new terms after 35 hours of CPU time on a 600MHz Alphastation. The Dickman *et al* [33] and Bonnier *et al* [34] results were reproduced in 5 seconds. To obtain the next term requires about  $10^3$  times more in computer time, which is not possible within availability of our computer resources.

## 2.5 Other formulations of series expansions

Beside the rate equation approach described in the previous three subsections, there are a number of other methods to obtain the series. Baram and Kutasov [32] and Baram and Fixman [35] used Ising spin notation and master equation to relate expansion coefficients to a counting problem of lattice animals as follows. The particle density is expanded as

$$\rho(t) = \sum_{n=1}^{\infty} (-1)^{n+1} a_n \frac{(1 - e^{-t})^n}{n!}. \quad (26)$$

For the nearest-neighbor exclusion model, the coefficient  $a_n$  is the number of connected lattice animals with  $n$  points that can grow from a single point. Unlike the rules embedded in the Eq. (16) for  $S(n)$  the new lattice animals are generated from perimeter sites only.

We can get this result from the rate equation point of view as follows. Let  $P(W)$  be the probability of a set of connected sites  $W$  for each of which a particle can be put in for sure. A large set  $G$  must be known to be empty. However, the correspondence between  $W$  and  $G$  is many to one. The rate equation for  $P(W)$  is then

$$\frac{dP(W)}{dt} = -mP(W) - \sum_x P(W \cup \{x\}), \quad (27)$$

where  $m = |W|$  is the number of sites in  $W$ , and  $x$  runs over the perimeter sites of  $W$  (for the nearest neighbor exclusion model). Let us transform  $t$  to  $y = 1 - e^{-t}$ , and  $Q(W, y) = (1 - y)^{-m} P(W, t)$ , then the new equation is

$$\frac{dQ(W)}{dy} = - \sum_{x, \text{ perimeter of } W} Q(W \cup \{x\}). \quad (28)$$

This naturally gives Eq. (26) and rule for  $a_n$ .

Dickman *et al* [33] gave an operator formulation of the master equation. The formal solution of the master equation is used to derive expansion rules identical to the rate equation approach. For the continuum problem, Schaaf and Talbot [29] gave small density expansions based on results in scaled particle theory [48]. The final result is equivalent to the time expansion, but the procedure is quite different. Consider the average fraction  $\phi$  of surface available to the center of a new disc,  $\phi = d\rho/dt$ . One has

$$\phi = 1 - S_1 + S_2 - S_3 + S_4 - \dots, \quad (29)$$

with

$$S_n = \frac{1}{n!} \int \int \dots \int dx_1 dx_2 \dots dx_n A_n(x_1, \dots, x_n) \rho^{(n)}(x_1, \dots, x_n), \quad (30)$$

where  $A_n(x_1, \dots, x_n)$  is the area common to the exclusion circle of  $n$  particles adsorbed at the positions defined by the vectors  $x_1, x_2, \dots, x_n$ ; i.e., it is the area of

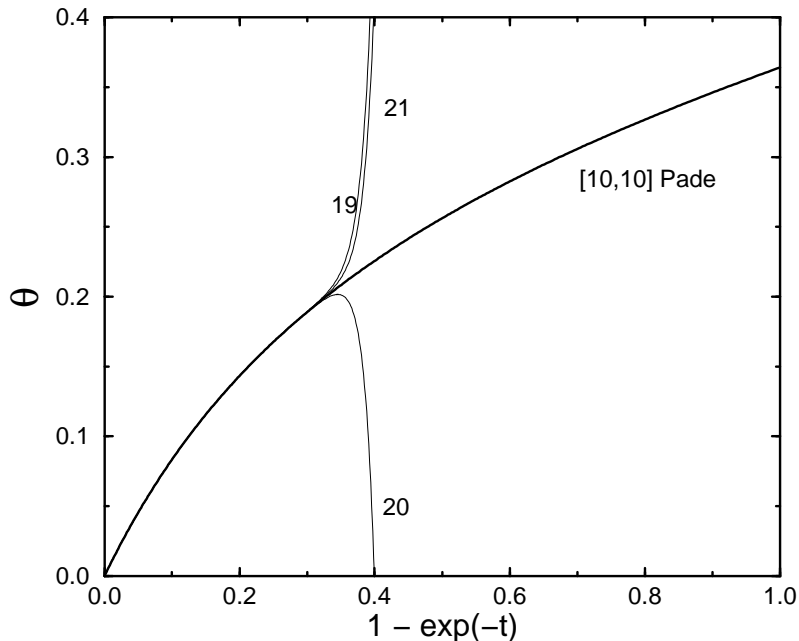


Figure 5: Series results for the RSA coverage on a square lattice of the monomer with nearest neighbor exclusion model. The curves labeled 19, 20, and 21 are the direct time series truncated to 19, 20, and 21 orders, respectively. The line labeled “[10,10] Padé” is  $N = D = 10$  Padé approximant in variable  $y$ , defined by Eq. (32), with  $b = 1.05$ . For convenience of viewing the whole range of  $t$ , we plot the curves with variable  $1 - \exp(-t)$ .

the set  $D(x_1) \cap D(x_2) \cdots \cap D(x_n)$ . The multi-variable function  $\rho^{(n)}(x_1, \cdots, x_n)$  is the general  $n$ -particle distribution function, which is proportional to the probability that a particle will be found in the elements of surface  $dx_1$  at  $x_1$ , a second in  $dx_2$  at  $x_2$ , etc. Schaaf *et al* observed that the leading order in a density expansion for  $S_n$  is equal to a corresponding equilibrium system. This allows them to find exact expression for  $S_n$  correct to third order in density [29, 49, 50, 51]. Tarjus *et al* [45] derived Kirkwood-Salsburg-like equations for  $\rho^{(n)}(x_1, \cdots, x_n)$ . From these equations, a diagrammatic expansion in density is obtained. Some what opposite in spirit to the rate equation approach, Given [44] formulates nonequilibrium problems as quenched, multi-species equilibrium problems. He also gave the topological reduction in graph expansion, showed clearly the parallel between RSA and equilibrium system. Caser and Hilhorst [52] presented series expansion directly for the jamming coverage. The approach is interesting, but the method is not very accurate.



## 2.6 Analysis of the series

The series obtained for the coverage in  $t$  has a finite radius of convergence, see Fig. 5. The fundamental question is whether we can give good approximation valid for the whole time domain  $t \in [0, \infty)$ . Although we do not have rigorous proof, the numerical procedure which we shall discuss below indicates a positive answer.

The standard technique of extending the radius of convergence is the Padé approximation method [22, 24]. Given a series  $f(x)$  to order  $L$ , we determine two polynomials  $P_N(x)$  and  $Q_D(x)$  of degree  $N$  and  $D$  respectively, such that

$$f(x) - \frac{P_N(x)}{Q_D(x)} = O(x^{L+1}), \quad N + D \leq L. \quad (31)$$

It is a powerful way of extending the domain of convergence of the original series. The polynomials  $P_N(x)$  and  $Q_D(x)$  with  $Q_D(x) = 1 + b_1x + \dots$  is usually determined uniquely for the given  $f(x)$ .

To accelerate the convergence further, new variables are introduced, e.g.,

$$y = 1 - \exp(-b(1 - e^{-t})). \quad (32)$$

The functional form is chosen in such a way so that the series in the new variable  $y$  most closely resembles the asymptotic behavior of the coverage  $\theta(t)$  at large  $t$ . For small  $t$ ,  $y$  is proportional to  $t$ . The above specific form is encouraged by the exact solution of the one-dimensional dimer problem. In fact, we have  $\theta = y$  with  $b = 2$  in such case (see Eq. (4)). The convergence among various Padé approximants is improved greatly by the transformation. This form of transformation works well for all lattice models that we have studied. For continuum models, Dickman *et al* [33] considered

$$y = 1 - \frac{1}{\sqrt{1 + bt}} \quad (33)$$

for the RSA of discs in two dimensions and

$$y = 1 - \frac{1 + \ln[1 + (b - 1)t]}{1 + bt} \quad (34)$$

for the oriented squares, which match the asymptotic law of  $t^{-1/2}$  (known as Feder's law [3]) and  $\log t/t$  law (Swendsen [8]), for discs and oriented squares, respectively.

Other methods of analysis were also used. For example, Fan and Percus [53] used exact results of solvable systems as reference systems which in some sense are close to the actual system to speed up the convergence. The coverage of the nearest neighbor exclusion model on a square cactus fractal lattice is [53]

$$\theta(z(t)) = \frac{1}{6} + \frac{1}{3}z - \frac{1}{6}(1 - z)^4, \quad (35)$$

where variable  $z$  is related to the original variable  $t$  by

$$1 - e^{-t} = 3 \int_0^z \frac{dz'}{1 + 2(1 - z')^3}. \quad (36)$$

We note that the coverage  $\theta$  is a truncated power series in  $z$  for the cactus system. The idea is that if we use the same variable  $z$ , relating  $t$  through Eq. (36), the nearest neighbor exclusion model on square lattice should have a series in  $z$  with much improved convergence.

Baram *et al* [32, 35] used Euler transform

$$y = \frac{1 - u}{c + 1 - u}, \quad u = e^{-t}, \quad c \approx 1, \quad (37)$$

and Levin convergence acceleration method [54] for the series analysis. It appears that the quality of the results is comparable to other methods.

The algebraic manipulations can be done with great ease by symbolic packages such as Maple or Mathematica. Mathematica contains function to find the Padé approximation of a series. The results of the analysis can then be plotted within the software. Here is an example of simple Mathematica code to form the series, do the transformation, call the Padé function, and finally evaluate the jamming coverage. The `SetPrecision[1.35,40]` command makes the subsequent computation in 40-digit precision.

```
<<Calculus`Pade`
maxord=17;
P[0] = 1;
P[1] = -4;
P[2] = 28;
P[3] = -268;
... (omitted)
P[17] = -6058617368871081964076;
theta = 1 - Sum[P[i]*t^i/i!, {i,0,maxord}] + 0[t]^(maxord+1);
b = SetPrecision[1.35,40];
f = theta /. t -> -Log[1 + Log[1-y]/b] + 0[y]^(maxord+2);
yinf = 1 - Exp[-b];
pd = Pade[f, {y, 0, 8, 8}];
thetainf = pd /. y -> yinf
```

The Padé approximant for the coverage of the dimer on square lattice is given in the `pd` variable as

$$\begin{aligned} & \left( 2.962963 y + 0.03206897 y^2 - 2.195246 y^3 - 1.073721 y^4 + 0.9207869 y^5 + 0.5556586 y^6 \right. \\ & \left. - 0.04386743 y^7 - 0.05303456 y^8 \right) / \left( 1 + 1.733045 y - 0.2568919 y^2 - 1.942572 y^3 \right. \\ & \left. - 0.5852424 y^4 + 0.7908992 y^5 + 0.4421557 y^6 - 0.0493306 y^7 - 0.0513337 y^8 \right), \quad (38) \end{aligned}$$

where  $y$  is given by Eq. (32) with  $b = 1.35$ . The result is stable against variation in  $b$ . Error can be estimated from the convergence of various Padé approximants.

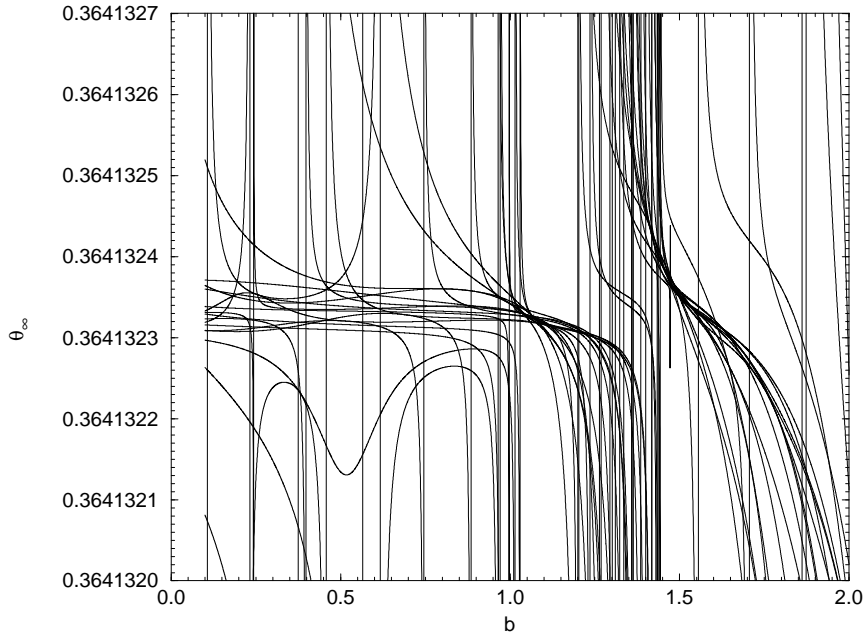


Figure 6: Padé approximant estimates for the jamming coverage  $\theta(\infty)$  as a function of the transformation parameter  $b$ , for the monomer RSA with nearest neighbor exclusion on a square lattice. The transformation is given by Eq. (32). (from ref. [36]).

The above Padé approximant is accurate to  $10^{-5}$  for all  $t \geq 0$ . Such a high degree of accuracy embedded in a simple formula is remarkable.

We set  $b$  to be a free variable so that when different orders of Padé approximants are applied to  $\theta(y)$ , a crossing region between different orders of Padé approximants is to be located so as to give a good estimate of jamming coverage  $\theta(\infty)$ . Some of the new series results and analyses are presented in Gan and Wang [36]. As an example, Fig. 6 shows the crossing region of Padé approximants of orders  $[N, D]$  with  $19 \leq N + D \leq 21$ ,  $D \geq 8$ ,  $N \geq 8$ , for the series of monomer RSA with nearest neighbor exclusion on a square lattice, giving an estimate of  $\theta(\infty) = 0.3641323(1)$ , where the last digit in parentheses denotes the uncertainty in the preceding digit. This estimate is in good agreement with the estimate of  $\theta(\infty) = 0.3641330(5)$  by Baram and Fixman [35]. Analyzing the series using the square cactus as a reference model [53], through the transformation Eq. (36), we obtain  $\theta(\infty) = 0.364132(1)$ , less accurate than that using transformation Eq. (32). All these estimates from the series analysis agree well with the simulation result of  $\theta(\infty) = 0.36413(1)$  [55].

The estimates for the jamming coverage on continuum systems are much less accurate, due to limited number of terms available in the series. In Fig. 7 we present the Padé estimates for the oriented squares as functions of the parameter  $b$ . Best convergence occurs around  $b = 1.3$ , given  $\theta(\infty) = 0.5623(4)$ . The additional new

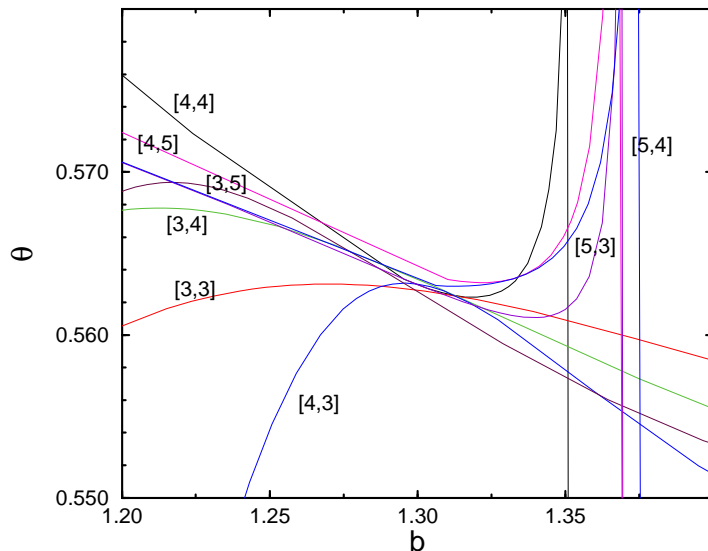


Figure 7: Padé approximant estimates for the jamming coverage  $\theta(\infty)$  as a function of the transformation parameter  $b$ , for the oriented square. The number  $[N, D]$  is the order of the Padé approximant. The transformation is given by Eq. (34).

terms do not improve the result of Dickman *et al* [33] very much.

In Table 3, we collect the results of jamming coverage compared with Monte Carlo results. It is clear, if the jamming coverage can be estimated with great accuracy, so is the whole function  $\theta(t)$ . The results for continuum models are less accurate. Nevertheless, we still obtain quite reasonable estimates.

### 3 Monte Carlo simulation

A large variety of RSA models have been simulated. Lattice models are easy to simulate with good accuracy. Random dimer filling is given by Nord and Evans [26] and Wang and Pandey [56]. Nearest neighbor exclusion models are simulated by Meakin *et al* [55]. Square blocks of  $n \times n$  are simulated by Nakamura [57], and by Barker and Grimson [58]. Square blocks with an emphasis of approaching to the continuum limit are studied by Privman *et al* [59].

On continuum, hard-disc system is simulated by Akeda and Hori [60], Finegold and Donnell [4], Tanemura [61], Feder [3], Hinrichsen *et al* [62], Meakin and Jullien [63], and Wang [64]. The oriented squares were of interest [60] because of Palásti conjecture [65], which says that the jamming coverage for the two-dimensional ori-

<i>Model</i>	<i>Series</i>		<i>Monte Carlo</i> $\theta(\infty)$
	<i>Order</i> $n$	<i>Padé</i> $\theta(\infty)$	
NN (square lattice)	21	0.3641323(1) [36]	0.36413(1) [55]
dimer (square lattice)	18	0.906823(2) [36]	0.906820(2) [56]
NN (honeycomb)	24	0.37913944(1) [36]	0.38(1) [28]
dimer (honeycomb)	22	0.8789329(1) [36]	0.87889 [26]
NNN (square lattice)	14	0.186985(2) [35]	0.186983(3) [59]
hard discs	5	0.5479 [33]	0.5470690(7) [64]
oriented squares	9	0.5623(4) [this work]	0.562009(4) [66]

Table 3: Some of the most accurate jamming coverages by series analysis and Monte Carlo computer simulation. NN stands for nearest neighbor exclusion, NNN for nearest and next neighbor exclusion. The order  $n$  is the highest known term in the time expansion of  $\theta(t)$ . The numbers in square brackets are references.

ented square is equal to the square of the one-dimensional line-segment jamming coverage. This conjecture turns out to be false [66].

Other more elaborated geometries are considered such as randomly oriented ellipses [67] and lines [68, 69], randomly oriented rectangles [70], and other anisotropic particles [71], spheroids [72], mixtures of different sizes [63, 73, 74]. The interests are the jamming coverage and the asymptotic laws for large time. Clearly, these complicated problems are difficult for systematic series expansions [51]. Lattice models with dimers on square lattice deposited with different probabilities in two orientations [75], with line segments [76], mixtures [77, 78, 79], and random walks [56, 80] are also studied.

We mention here briefly two related generalizations of standard RSA. The first of these is multilayer RSA [81]. The jamming densities as a function of the height show interesting power-law behavior [82]. The second generalization is RSA with diffusional relaxation [40, 83, 84, 85, 86, 87, 88]. When diffusional relaxations are introduced, many of the intrinsic properties of RSA changes. Most of these generalized models are studied by Monte Carlo computer simulation.

### 3.1 Simple algorithms

Monte Carlo simulation method has the advantage of very little programming investment, quick and robust results. Random sequential adsorption, especially lattice models, can be simulated on a computer rather easily. The basic variables (declared as an array) are the occupations of the lattice sites. At each time step, a site  $x$  is picked at random, if some neighborhood  $D(x)$  is empty, we put down the particle by reset the array values in these entries of involved sites. Note that one is simulating a time-discretized version of the RSA model, while the rate equation approach considers continuous time. The discretization step is  $1/L^d$  where  $L$  is the linear dimension

of the system. However, discretization effect is unimportant since we can simulate very large systems easily.

With continuum models, since we can not have occupation variables like the lattice models, more tricks are needed for efficiency. The coordinates of the particles are stored to register the locations. To speed up the checking for overlapping, “coarse-grained occupation variables” are needed to indicate where are the particles in a given range, a technique borrowed from molecular dynamics simulation. For example, in RSA of discs, the total  $L \times L$  surface area is partitioned into regions of squares of size  $1 \times 1$ . A disc at  $(x, y)$  belongs to the unit square at  $(\lfloor x \rfloor, \lfloor y \rfloor)$ , where the notation  $\lfloor x \rfloor$  represents the floor or integer part of  $x$ . An array of linked lists of disc coordinates is used to represent the deposited discs. With this data structure, it is suffice just to check the discs located at the center and eight surround squares for overlaps.

The above simple methods have a severe shortcoming that the study of late-stage process is very time-consuming. When the jamming configuration is about to be reached, much of the area is blocked. Only tiny disconnected regions are available for further deposition. Since we choose the sites at random with a uniform probability distribution, the available sites are hard to find. More advanced methods cleverly discover these regions and suggest deposition only in regions which are potentially possible for adsorption.

## 3.2 Event driven algorithms

First we consider the lattice models. On a lattice, since there are only finite number (of order  $N = L^d$ ) of possibilities for deposition, each with equal probability in the original definition of the model, we can classify the deposition possibilities as possible and impossible attempts. For example, for the nearest neighbor exclusion model, each site is associated with a deposition attempt. The possible sites are those with center and four neighbors empty; the impossible sites are those with any one of the five sites occupied. Let us assume that we have  $N_a$  possibilities for the available type and  $N_i$  for the impossible type. Clearly,  $N_a + N_i = N$ . In the normal simulation, we hit the first available type with probability  $p = N_a/N$  and other type with  $1 - p = N_i/N$ . Consider a total of  $k$  attempts such that the first  $k - 1$  failed to deposit a particle because one hits already blocked sites and the  $k$ -th attempt is successful and is deposited. What is the probability that such an event occurs? Each failed attempt occurs with probability  $(1 - p)$ , so  $k - 1$  consecutive fails have probability  $(1 - p)^{k-1}$ . Since each failed attempt does not change the current state of the system, the next attempt is totally independent of the previous attempts. The successful attempt has probability  $p$  so the total probability is

$$P_k = p(1 - p)^{k-1}, \quad k = 1, 2, \dots \quad (39)$$

Imagine that we do not actually do the  $k-1$  failed attempts, and pick one at random from the available sites and deposit the particle. From the above discussion, this is equivalent to  $k$  attempts in units of the original time scale. However,  $k$  is not a definite number, rather it follows the probability distribution, Eq. (39).

Event-driven type of algorithms was invented long-time ago for the simulation of Ising models [89], which is known as N-fold way. An event-driven RSA algorithm [64, 66] on lattice is as follows: pick deposition site from the list of available sites at random. Increase the time  $t$  by  $k/L^d$  ( $L^d$  attempts are usually defined as unit time). Update the configuration and the list.

The random integer  $k$  can be generated by transformation method as follows:

$$k = 1 + \left\lfloor \frac{\ln \xi}{\ln(1-p)} \right\rfloor, \quad (40)$$

where  $\xi$  is a uniformly distributed random number between 0 and 1. Some programming efforts are needed to update the list efficiently. After one deposition, not only the current site but also some other sites in the neighborhood of the current site are no longer available. This should be correctly reflected in the list. The deposition also changes the value  $p$ .

Perhaps the best application of the technique to lattice model is the RSA of polymer chains [56]. Due to a large number of conformational states of polymer chains, the deposition becomes very slow in the late stage. An event-driven method is, therefore, essential to obtain long-time results. This is accomplished by identifying the early part of growing chains, i.e., the partial chains and then classifying them periodically as “available” or “not available” for the deposition in an iterative fashion. The subsequent depositions are then made starting from the available partial chains choosing at random. The list of the partial chains is limited by the available computer memory and governs the speed of the program. It appears that there is an optimal list size for a given length of a chain.

Highly accurate Monte Carlo simulation results were obtained for oriented squares [66] and for discs [64] on two-dimensional continuum. In the RSA simulation of discs, we incorporated two important ideas: (1) divide the surface into small squares and make deposition attempts only on squares that are not completely blocked; (2) systematically reduce the sizes of the small squares after some number of attempts and re-evaluate the availability of the squares.

In this more elaborate method, we make attempts only on squares which are potentially possible for depositions. Thus the core part is an algorithm which identifies correctly whether a square is available for deposition. Since the diameter of the discs is  $\sigma = 1$ , each disc excludes an area of circle of radius  $\sigma$  for further deposition. If some area is completely covered by a union of the exclusion zones of discs, that area is not available for deposition. We begin by classifying all the squares of  $a \times a$  with  $a = 1$  as available or unavailable squares. The available squares are put on a

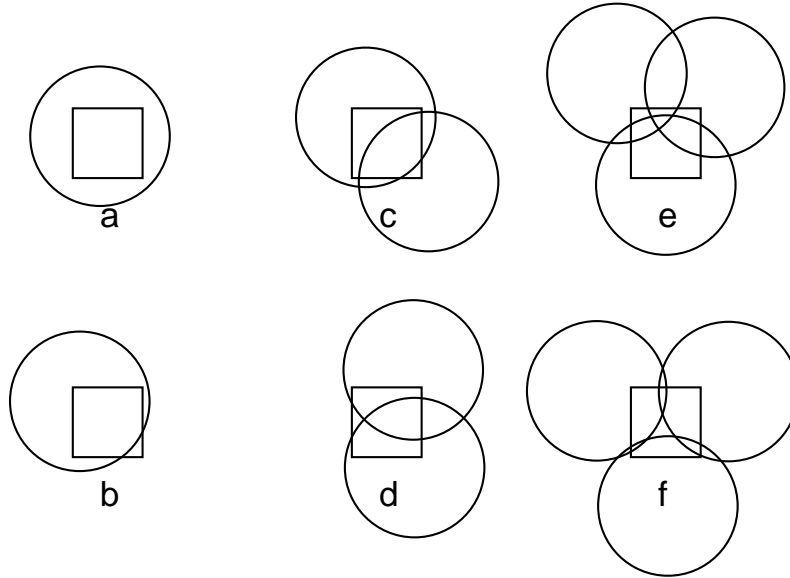


Figure 8: The six different situations for discs covering or not covering a square.

list. Deposition trials are taken only on the squares in the list, i.e., a square in the list is chosen at random, deposition is attempted with a uniform probability over the square. After certain number of trials (we used  $5 \times 10^5$ ), we rebuild the list, now with squares of size  $(a/2) \times (a/2)$ , checking only those squares on the old list. Each old square is subdivided into 4 smaller squares. This shrinking of the basic squares helps to locate even extremely small available regions. They will be hit with very small probability if the area is always  $1 \times 1$ . Because of integer overflow, the size of the squares is not allowed to go arbitrarily small, but the shrinking is stopped at  $a = 2^{-15}$ . Thus the smallest square has an area of  $2^{-30} \approx 10^{-9}$ .

For the standard RSA algorithm, each trial increases the time  $t$  by  $1/A$ , where  $A = L^2$  is the area of the total surface. In the even-driven algorithm, where only the potentially successful depositions are tried, the clock must tick faster in order to compensate for not making attempts in the completely unsuccessful area. The time increment for each trial on the available squares is given by  $k/A$  with  $k$  generated using Eq. (40), with  $p$  being the ratio of the area on which we try our deposition to the total area; it is equal to  $a^2/L^2$  times the number of available squares.

An important piece of code of our RSA simulation program is the identification of the squares which are fully covered by the excluded area of discs. For these squares we are sure that depositions on them will be unsuccessful, and thus they will not be on the list of candidates for trials.

The algorithm that we have devised is as follows. Written as a C programming



language function, it returns a nonzero value if the square is fully covered and a value 0 otherwise. Part (1) to (5) is executed in the order given.

1. Find relevant discs to the current square. A disc is relevant if the square overlaps with the excluded region of the disc. Note that a disc has a diameter  $\sigma$  and its excluded region is a concentric circle of radius  $\sigma$ .
2. If all of the four vertices of the square are inside a single-disc excluded region, then it is already fully covered (Fig. 8a). Function returns with value 1.
3. For a full coverage, each vertex of the square must be at least in one of the excluded region of the relevant discs. If any one of the vertices is not covered at all by any disc, then the square is not fully covered (Fig. 8b). Function returns with value 0.
4. At this point, at least two discs are involved if the function is not returned. Mapping the edges of the square to a one-dimensional line between 0 and 4, we find out all the line segments which are covered by the excluded region of discs. If the four edges of the square are completely covered by the discs, and we have exactly two discs, then the square is fully covered (Fig. 8c), function returns with value 2. If there are segments not covered by discs, then we know that the square is not fully covered (Fig. 8d). Function returns with value 0.
5. If the function is not returned, we know that there are at least three discs. Even if all the edges are covered, the square can still contain uncovered area if three or more discs are involved. Three or more discs can form holes. To make the last check, the coordinates of the intersection points of circles (with radius  $\sigma$ ) are calculated. In order for the interior of the square to be covered, all the intersection points of any pair of discs which lie inside or on the square edges must be covered by a third disc. Return with the number of relevant discs if the above condition is satisfied (Fig. 8e); return value 0 if not (Fig. 8f).

The order of various checks is arranged in such a way so that the most frequent and easy situations are checked first. Even though the worst case computational complexity goes as  $n^2$ , where  $n$  is the number of relevant discs, a definite conclusion can be made typically much earlier. Using this algorithm, Wang [64] obtained accurate jamming coverage  $\theta(\infty) = 0.5470690(7)$  and confirmed to a high accuracy the Feder's asymptotic law  $\theta(t) \approx \theta(\infty) - ct^{-1/2}$ .

## 4 Conclusion

We introduced the method of series expansions for both lattice models and continuum models. The computation of the series for the lattice model can be reduced to

a counting problem. An efficient implementation requires full use of the symmetry of the problem. For continuum models, systematic expansion in terms of a class of graphs are available. Both the problem of reducing labeled graphs to unlabeled graphs and of computing the cluster integrals are computationally difficult problems. Thus, the series for continuum systems are rather short. The series can be analyzed through variable transformation and Padé approximation. Monte Carlo simulation method is versatile, and implementation is straightforward. However, efficient algorithms are available with more sophisticated data structures. The challenge to the series expansion and efficient Monte Carlo simulation for RSA is to apply to more complicated models which may describe better real experiment situations.

## Acknowledgements

The author thanks R. Dickman, C. K. Gan, R. Hilfer, P. Nielaba, and V. Privman. Many of the original results presented in this article were obtained together with them in fruitful collaborations. He also thanks E. C. Chang for discussion on graph algorithms.

## References

- [1] P. J. Flory, *J. Am. Chem. Soc.* 61 (1939) 1518.
- [2] A. Renyi, *Publ. Math. Inst. Hung. Acad. Sci.* 3 (1958) 109; Selected Transl. *Math. Stat. Prob.* 4 (1963) 203.
- [3] J. Feder, *J. Theor. Biol.* 87 (1980) 237.
- [4] L. Finegold and J. T. Donnell, *Nature*, 278 (1979) 443.
- [5] G. Y. Onoda and E. G. Liniger, *Phys. Rev. A* 33 (1986) 715.
- [6] V. Privman, J.-S. Wang, and P. Nielaba, *Phys. Rev. B.* 43 (1991) 3366.
- [7] Y. Pomeau, *J. Phys. A: Math. Gen.* 13 (1980) L193.
- [8] R. H. Swendsen, *Phys. Rev. A*, 24 (1981) 504.
- [9] P. Viot and G. Tarjus, *Europhys. Lett.* 13 (1990) 295.
- [10] G. Tarjus and P. Viot, *Phys. Rev. Lett.* 67 (1991) 1875.
- [11] J. W. Evans, *Rev. Mod. Phys.* 65 (1993) 1281.
- [12] M. C. Bartelt and V. Privman, *Int. J. Mod. Phys. B* 5 (1991) 2883.
- [13] J. J. Ramsden, *J. Stat. Phys.* 73 (1993) 853.
- [14] E. S. Page, *J. R. Stat. Soc., B* 21 (1959) 364.
- [15] J. K. Mackenzie, *J. Chem. Phys.* 37 (1962) 723.
- [16] E. R. Cohen and H. Reiss, *J. Chem. Phys.* 38 (1963) 680.
- [17] J. J. Gonzalez, P. C. Hemmer, and J. S. Høye, *Chem. Phys.* 3 (1974) 228.
- [18] B. Bonnier, D. Boyer, and P. Viot, *J. Phys. A: Math. Gen.* 27 (1994) 3671.
- [19] J. W. Evans, *J. Math. Phys.* 25 (1984) 2527.
- [20] A. Baram and D. Kutasov, *J. Phys. A: Math. Gen.* 25 (1992) L493; *J. Phys. A: Math. Gen.* 27 (1994) 3683.
- [21] Y. Fan and J. K. Percus, *J. Stat. Phys.* 66 (1992) 263.
- [22] A. J. Guttmann, in “Phase Transitions and Critical Phenomena,” Vol. 13. edited by C. Domb and J. L. Lebowitz, Academic, New York, 1989.
- [23] C. Domb, “The Critical Point,” Taylor & Francis, London, 1996.

- [24] G. A. Baker and P. Graves-Morris, "Padé Approximants, Encyclopedia of Mathematics and its Applications, Vols. 13 and 14. Addison-Wesley, Reading, 1981. G. A. Baker, "Quantitative Theory of Critical Phenomena," Academic Press, Boston, 1990.
- [25] J. W. Evans and R. S. Nord, *J. Stat. Phys.* 38 (1985) 681.
- [26] R. S. Nord and J. W. Evans, *J. Chem. Phys.* 82 (1985) 2795.
- [27] P. Schaaf, J. Talbot, H. M. Rabeony, and H. Reiss, *J. Phys. Chem.* 92 (1988) 4826.
- [28] B. Widom, *J. Chem. Phys.* 44 (1966) 3888; 58 (1973) 4043.
- [29] P. Schaaf and J. Talbot, *Phys. Rev. Lett.* 62 (1989) 175.
- [30] D. K. Hoffman, *J. Chem. Phys.* 65 (1976) 95.
- [31] J. W. Evans, *Physica A* 123 (1984) 297; *J. Chem. Phys.* 87 (1989) 3038; *Phys. Rev. Lett.* 62 (1989) 2624.
- [32] A. Baram and D. Kutasov, *J. Phys. A: Math. Gen.* 22 (1989) L251.
- [33] R. Dickman, J.-S. Wang, and I. Jensen, *J. Chem. Phys.* 94 (1991) 8252.
- [34] B. Bonnier, M. Hontebeyrie, and C. Meyers, *Physica A*, 198 (1993) 1.
- [35] A. Baram and M. Fixman, *J. Chem. Phys.* 103 (1995) 1929.
- [36] C. K. Gan and J.-S. Wang, *J. Chem. Phys.* 108 (1998) 3010.
- [37] K. J. Vette, T. W. Orent, D. K. Hoffman, and R. S. Hansen, *J. Chem. Phys.* 60 (1974) 4854.
- [38] C. K. Gan and J.-S. Wang, *J. Phys. A: Math. Gen.* 29 (1996) L177.
- [39] T. H. Cormen, C. E. Leiserson, and R. L. Rivest, "Introduction to Algorithms," the MIT Press, Cambridge, 1990.
- [40] C. K. Gan and J.-S. Wang, *Phys. Rev. E.* 55 (1997) 107.
- [41] J.-S. Wang and C. K. Gan, *Phys. Rev. E.* 57 (1998) 6548.
- [42] J. P. Hansen and I. R. McDonald, "Theory of Simple Liquids," Academic Press, London, 1976.
- [43] G. E. Uhlenbeck and G. E. Ford, in "Studies in Statistical Mechanics," Part B, Vol. 1, edited by J. de Boer and G. E. Uhlenbeck North-Holland, Amsterdam, 1962; H. L. Friedman, "A Course in Statistical Mechanics," Chapter 6, Prentice-Hall, Englewood Cliffs, 1985.

- [44] J. A. Given, *Phys. Rev. A* 45 (1992) 816.
- [45] G. Tarjus, P. Schaaf, and J. Talbot, *J. Stat. Phys.* 63 (1991) 167.
- [46] W. G. Hoover and A. G. De Rocco, *J. Chem. Phys.* 36 (1962) 3141.
- [47] B. D. McKay, *J. Algorithms*, 26 (1998) 306.
- [48] H. Reiss, H. L. Frisch, and J. L. Lebowitz, *J. Chem. Phys.* 31 (1959) 369.
- [49] P. Schaaf and J. Talbot, *J. Chem. Phys.* 91 (1989) 4401.
- [50] J. Talbot, P. Schaaf, and G. Tarjus, *Mol. Phys.* 72 (1991) 1397.
- [51] S. M. Ricci, J. Talbot, G. Tarjus, and P. Viot, *J. Chem. Phys.* 97 (1992) 5219.
- [52] S. Caser and H. J. Hilhorst, *J. Phys. A: Math. Gen.* 27 (1994) 7969; *J. Phys. A: Math. Gen.* 28 (1995) 3887.
- [53] Y. Fan and J. K. Percus, *Phys. Rev. Lett.* 67 (1991) 1677; *Phys. Rev. A*, 44 (1991) 5099.
- [54] D. Levin, *J. Comput. Math.* 3 (1973) 371.
- [55] P. Meakin, J. L. Cardy, E. Loh, Jr., and D. J. Scalapino, *J. Chem. Phys.* 86 (1987) 2380.
- [56] J.-S. Wang and R. B. Pandey, *Phys. Rev. Lett.* 77 (1996) 1773.
- [57] M. Nakamura, *J. Phys. A: Math. Gen.* 19 (1986) 2345.
- [58] G. C. Barker and M. J. Grimson, *Mol. Phys.* 63 (1988) 145; *J. Phys. A: Math. Gen.* 20 (1987) 2225.
- [59] V. Privman, J.-S. Wang, and P. Nielaba, *Phys. Rev. B*, 43 (1991) 3366.
- [60] Y. Akeda and M. Hori, *Nature*, 254 (1975) 318; *Biometria*, 63 (1976) 361.
- [61] M. Tanemura, *Ann. Inst. Stat. Math.* 31 (1979) 351.
- [62] E. L. Hinrichsen, J. Feder, and T. Jøssang, *J. Stat. Phys.* 44 (1986) 793.
- [63] P. Meakin and R. Jullien, *Phys. Rev. A*, 46 (1992) 2029; *Physica A* 187 (1992) 475.
- [64] J.-S. Wang, *Int. J. Mod. Phys. C*, 5 (1994) 707.
- [65] I. Palásti, *Magy. Tud. Akad. Mat. Kut. Intéz. Közl.* 5 (1960) 353.
- [66] B. J. Brosilow, R. M. Ziff, and R. D. Vigil, *Phys. Rev. A* 43 (1991) 631.

- [67] J. Talbot, G. Tarjus, and P. Schaaf, Phys. Rev. A 40 (1989) 4808.
- [68] J. D. Sherwood, J. Phys. A: Math. Gen. 23 (1990) 2827.
- [69] R. M. Ziff and R. D. Vigil, J. Phys. A: Math. Gen. 23 (1990) 5103.
- [70] R. D. Vigil and R. M. Ziff, J. Chem. Phys. 91 (1989) 2599; 93 (1990) 8270.
- [71] P. Viot, G. Tarjus, S. M. Ricci, and J. Talbot, J. Chem. Phys. 97 (1992) 5212.
- [72] Z. Adamczyk and P. Weroński, J. Chem. Phys. 105 (1996) 5562.
- [73] J. Talbot and P. Schaaf, Phys. Rev. A 40 (1989) 422.
- [74] G. Tarjus and J. Talbot, J. Phys. A: Math. Gen. 24 (1991) L913.
- [75] M. J. de Oliveira, T. Tomé, and R. Dickman, Phys. Rev. A, 46 (1992) 6294.
- [76] S. S. Manna and N. M. Švrakić, J. Phys. A 24 (1991) L671.
- [77] N. M. Švrakić and M. Henkel, J. Phys. I, 1 (1991) 791.
- [78] B. Bonnier, Europhys. Lett. 18 (1992) 297.
- [79] R. S. Sinkovits and R. B. Pandey, J. Stat. Phys. 74 (1994) 457.
- [80] L. Budinski-Petković and U. Kozmidis-Luburić, Phys. Rev. E. 56 (1997) 6904; Physica A 236 (1997) 211; Physica A 262 (1999) 388.
- [81] P. Nielaba, V. Privman, and J.-S. Wang, J. Phys. A: Math. Gen. 23 (1990) L1187; and in *Computer Simulation Studies in Condensed-Matter Physics VI*, D. P. Landau, K. K. Mon, H.-B. Schüttler, eds., Springer Proceedings in Physics, Vol. 76, p. 143, Springer-Verlag, Heidelberg, 1993.
- [82] R. Hilfer and J.-S. Wang, Phys. A: Math. Gen. 24 (1991) L389.
- [83] V. Privman and P. Nielaba, Europhys. Lett. 18 (1992) 673.
- [84] V. Privman and M. Barma, J. Chem. Phys. 97 (1992) 6714.
- [85] J.-S. Wang, P. Nielaba, and V. Privman, Mod. Phys. Lett. B 7 (1993) 189; Physica A, 199 (1993) 527.
- [86] G. G. Pereira and J.-S. Wang, Physica A 242 (1997) 347.
- [87] B. Bonnier, Phys. Rev. E. 56 (1997) 7304.
- [88] E. Eisenberg and A. Baram, Europhys. Lett. 44 (1998) 168.
- [89] A. B. Bortz, M. H. Kalos, and J. L. Lebowitz, J. Comput. Phys. 17 (1975) 10.